

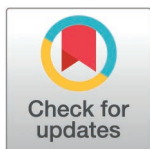
RESEARCH ARTICLE

# Neural complexity in preterm infants is predicted by developmental variables

Lorenzo Semeia <sup>1,2\*</sup>, Amer Zaylaa <sup>1,3</sup>, Dimitrios Metaxas <sup>1,4</sup>, Mina Nourhashemi<sup>5</sup>, Mahdi Mahmoudzadeh<sup>5</sup>, Andreas L. Birkenfeld<sup>1,3</sup>, Katrin Sippel<sup>1</sup>, Pedro A. M. Mediano <sup>6</sup>, Hubert Preissl<sup>1,3,7,8</sup>, Fabrice Wallois<sup>5</sup>, Joel Frohlich <sup>1,3,9\*</sup>

**1** IDM/fMEG Center of the Helmholtz Center Munich at the University of Tübingen, Eberhard Karls University of Tübingen, German Center for Diabetes Research (DZD), Tübingen, Germany, **2** Graduate Training Centre of Neuroscience, International Max Planck Research School, Eberhard Karls University of Tübingen, Tübingen, Germany, **3** Internal Medicine IV, Department of Diabetology, Endocrinology, Nephrology, University Hospital Tübingen, Tübingen, Germany, **4** Graduate Training Centre of Neuroscience, Eberhard Karls University of Tübingen, Tübingen, Germany, **5** INSERM U1105, GRAMFC, Université de Picardie Jules Verne, Amiens, France, **6** Department of Computing, Imperial College London, London, United Kingdom, **7** Department of Pharmacy and Biochemistry, Interfaculty Centre for Pharmacogenomics and Pharma Research, Eberhard Karls University of Tübingen, Tübingen, Germany, **8** German Center for Mental Health (DZPG), Partner Site Tübingen, Tübingen, Germany, **9** Institute for Advanced Consciousness Studies, Santa Monica, California, United States of America

\* [Lorenzo.Semeia@med.uni-tuebingen.de](mailto:Lorenzo.Semeia@med.uni-tuebingen.de) (LS); [jfneuro@pm.me](mailto:jfneuro@pm.me) (JF)



 OPEN ACCESS

**Citation:** Semeia L, Zaylaa A, Metaxas D, Nourhashemi M, Mahmoudzadeh M, Birkenfeld AL, et al. (2025) Neural complexity in preterm infants is predicted by developmental variables. *PLOS Complex Syst* 2(10): e0000056. <https://doi.org/10.1371/journal.pcsy.0000056>

**Editor:** Morten Gram Pedersen, University of Padova: Università degli Studi di Padova, ITALY

**Received:** November 19, 2024

**Accepted:** June 23, 2025

**Published:** October 6, 2025

**Peer Review History:** PLOS recognizes the benefits of transparency in the peer review process; therefore, we enable the publication of all of the content of peer review and author responses alongside final, published articles. The editorial history of this article is available here: <https://doi.org/10.1371/journal.pcsy.0000056>

**Copyright:** © 2025 Semeia et al. This is an open access article distributed under the terms of the [Creative Commons Attribution License](https://creativecommons.org/licenses/by/4.0/), which permits unrestricted use, distribution,

## Abstract

Neural complexity, measured as the entropy of noninvasively recorded electrophysiological signals, evolves with age in early infancy, differentiates between typical and atypical development, and likely serves as a surrogate marker of brain maturation. However, the reason for this evolution of neural entropy in early infant development remains unclear. To understand this evolution, we measured the proportion of time that the infant brain spent in a bursting pattern of activity and related this activity pattern to the neural complexity (i.e., entropy or entropy rate). Additionally, we sought to predict neural complexity using each infant's gestational age and to replicate sex-related complexity differences previously reported in age-equivalent fetuses. Four distinct complexity estimator algorithms – Lempel-Ziv (LZ) complexity, multiscale entropy (MSE), complexity via state-space entropy rate (CSER), and context tree weighting (CTW) – were applied to 8-channel infant electroencephalogram (EEG) recordings in 28 preterm infants (27–34 weeks gestational age). To explore factors influencing signal complexity, we modeled relationships between complexity estimates, on the one hand, and spontaneous activity transients, gestational age, and sex, on the other hand. We calculated channel-averages for each complexity estimate separately, as derived either from entire EEG recordings or separately from burst and interburst periods. Our results suggest that increased EEG signal continuity with maturation may drive increases in neural complexity as quiescent periods subside. Additionally, our results largely recapitulate previous findings linking neural complexity to biological sex in third-trimester fetuses. We also observed unexpected differences between entropy

and reproduction in any medium, provided the original author and source are credited.

**Data availability statement:** The raw EEG data underlying our results cannot be made publicly available because research consent forms signed by parents did not explicitly authorize infant data sharing beyond the immediate consortium. Therefore, we are legally and ethically constrained from sharing the EEG data underlying our results. To facilitate reproducibility to the greatest extent possible, neural complexity measures (entropy and entropy rate values from all algorithms used in this study) and the aperiodic exponent for each participant have been deposited on the project's Open Science Framework (OSF) page, alongside other variables such as percent spontaneous activity transients (pSAT), Apgar score at 1 minute after birth, sex, birth weight, gestational age at time of EEG recording, and gestational age at birth of each infant. These data can be downloaded from OSF [<https://osf.io/d4x53/files/osfstorage>] and form the necessary dataset needed to reproduce our statistical analyses and figures within the restrictions mentioned above.

**Funding:** This study was conducted with the support of the Procope Mobility program of the French Embassy in Germany, which is designed to enhance scientific cooperation between France and Germany. The work was also partially funded by the ANR-DFG French-German collaboration (PR 496/11-1). We also thank the International Max Planck Research School for the Mechanisms of Mental Function and Dysfunction (IMPRS-MMFD) and the Joachim Herz Foundation. D.M. was supported by IKY-State Scholarship Foundation through the 'in memory of Maria Zaousi' scholarship program. The funders had no role in study design, data collection and analysis, decision to publish, or preparation of the manuscript.

**Competing interests:** J.F. receives consulting fees from IAMA Therapeutics and funding from the Bial Foundation, both unrelated to this project. M.M. is a principal scientist at Neurocrine Biosciences since July 2022 and Scientific Advisor at Seenal Imaging since January 2018, both positions unrelated to this project. M.N. is a research scientist at Powell Mansfield since 2025, also unrelated to this project. These disclosures do not pose any conflict of interest regarding the work undertaken for this publication.

rate results obtained using CSER (a newer algorithm) and older algorithms. These findings support further research into neural complexity as a potential predictor of clinical outcomes in infants at high risk for neurodevelopmental disorders.

## Author summary

There are currently two languages for describing the evolution of neural dynamics in the first weeks of human life: the qualitative language of tracé discontinu – electrophysiological patterns of bursting and quiescent activity – and the quantitative language of signal entropy, or the number of ways in which discrete states of a neural signal can be arranged. Here, we attempt to unify these two languages by measuring bursting activity in terms of spontaneous activity transients and using these measurements, alongside other developmental variables, to predict the neural entropy or entropy rate (collectively referred to as complexity) in premature infants. A further goal of our analysis was to understand why neural complexity changes week-by-week in the human infant brain. Our results suggest that this change is driven by qualitative changes in infant neural activity, which grows more continuous with age. Consistent with previous work, we also uncovered associations between biological sex and neural complexity in the earliest weeks of life. By revealing the developmental drivers of neural complexity in premature infants, we not only provide a useful context for understanding the evolution of infant neural complexity but, also, we lay the groundwork for future efforts toward practical, predictive biomarkers of developmental outcomes rooted in neural complexity features.

## 1. Introduction

The human brain is characterized by complex and nonlinear dynamics [1–3], yet the extent to which neural complexity tracks developmental processes remains unclear, particularly in the earliest stages of human development. More broadly, the complexity of neural signals (i.e., the richness or diversity of brain activity) has delivered promising results in studies of cognitive processes [4–7] and disorders such as Parkinson's [8], epilepsy [9], anesthesia [10], and Alzheimer's [11]. Most relevantly for our purposes, neural complexity has been used in developmental contexts as an indicator of brain maturation and developmental delays [12,13], as well as a predictor of autism spectrum disorder diagnosis [14] or familial autism risk [15]. Several studies of neural complexity in early development have focused on preterm infants, i.e., those born before the 37<sup>th</sup> week of gestation, which account for approximately 11% of all livebirths worldwide [16] and are at heightened risk of negative developmental outcomes, which manifest in neurological, psychiatric, or motor domains [17–20].

Many methods of estimating neural complexity exist [1–3], most of which reflect the entropy of neural signals, i.e., the number of ways in which states of a signal can be arranged, or the entropy rate, which, unlike entropy, is sensitive to shuffling the

**Abbreviations:** CSER, Complexity via state-space entropy rate; CTW, Context tree weighting; EEG, Electroencephalography; FDR, False Discovery Rate; GA, weeks of Gestational Age; IBIs, inter-burst intervals; LZ, Lempel-Ziv compressibility; MSE, Multiscale Entropy; SAT, Spontaneous Activity Transient; pSAT, proportion of time points detected as SAT over the total duration of the dataset.

order of signal states. In neonatal electroencephalography (EEG), neural complexity differs between sleep stages, with higher complexity during active sleep (analogous to rapid eye movement sleep in adults) compared to quiet sleep (analogous to non-rapid eye movement sleep in adults) [21–23]. This suggests that, even in earliest stages of life, neural complexity may track the brain's capacity for information processing, which is greater during wakefulness. Additionally, elevated complexity is present in full-term infants relative to preterm infants of comparable gestational age (GA) [24], suggesting the potential of neural complexity as a clinical biomarker sensitive to early developmental risk. Along these lines, preterm newborns who underwent a skin-to-skin maternal care intervention or “kangaroo care” also show higher EEG-derived complexity compared to preterm newborns without the same intervention at comparable GA [22,25], further implying potential for neural complexity as a clinical biomarker or, e.g., a surrogate endpoint in clinical trials.

In order to further develop neural complexity as a prognostic biomarker of long-term outcomes in preterm infants, it is essential to understand how neural complexity evolves during the perinatal period and early infancy. When applied to spontaneous EEG signals, measures of neural complexity generally increase with GA in preterm infants [21], an intuitive result given concurrent increases in anatomical complexity [26]. Indeed, neural complexity continues to increase until late adolescence [12,27], hinting at an overarching developmental trajectory whereby complexity may track maturation from gestation to adulthood.

However, recent work has added a kink to this story. Magnetoencephalography (MEG) findings have demonstrated that neural complexity actually *decreases* with GA in auditory evoked neural signals recorded from both fetuses and newborns [28]. The same work also uncovered unexpected dependencies of MEG signal complexity on fetal sex, highlighting the difficulty of interpreting neural complexity during the perinatal period. In short, neural complexity appears to depend not only on gestational age, as has already been demonstrated by a number of studies [21,22,29], but likely also on sex and recording technique (e.g., EEG versus MEG, spontaneous versus sensory evoked recordings, etc.).

The foregoing fetal MEG findings have yet to be reproduced using EEG in preterm infants. At the same time, because the fetal MEG data in the foregoing study were event related, the findings did not address whether neural complexity is influenced by cortical events which are largely unique to spontaneous neural dynamics in the perinatal brain. These include quiescent periods, also known as inter-burst intervals (IBIs), separated by bursts of neural activity known as spontaneous activity transients (SATs). Both activity patterns are developmentally relevant, as SATs seem to be needed for neural wiring and network formation during brain development [30–32], and IBIs are common in neonates who are small for their gestational age when compared to peers appropriate for their age [33]. To fill this gap in existing knowledge, we computed neural complexity from EEG recordings in preterm infants using developmental variables, fitting separate models for EEG data recorded during bursts and between bursts. We chose preterm infants as subjects because SATs and IBIs can be easily recorded in their EEG signals; by comparison, fetal MEG is usually restricted to event-related activity due to its low signal-to-noise ratio [34].

Specifically, we examined differences in neural signal complexity between burst and interburst periods using a dataset from Nourhashemi et al. [35]. We hypothesized that 1) neural complexity in our group of preterm neonates would increase with GA, 2) neural complexity would be lower in boys than in girls, following previous work [28], and 3) SATs influence, and thus predict, neural complexity estimates, with higher neural complexity during SATs as compared with IBIs. Furthermore, to ensure that neural complexity is not better explained by other developmental variables, we addressed these hypotheses using a stepwise linear modeling approach which also considers alternative predictors.

## 2. Methods

### 2.1. Infants and recordings

The infant details, recordings and datasets are described in Nourhashemi et al. [35]. In short, the study recruited 32 preterm neonates between 27–35 weeks of GA whose EEG data were recorded while they rested in a supine position. The ethics committee of the Amiens University Hospital approved this study (CPP Nord-Ouest II-France IDRCEB-2008-A00704-51). Parents gave their informed consent in accordance with the Declaration of Helsinki, and agreed to their infant's data being used for further research. The EEG electrodes were placed on the infant's scalp to record spontaneous neural data (for further details on the recording system, see Nourhashemi et al. [35]). For the current analysis, we included all available EEG channels (eight in total). Electrodes were placed according to the 10–20 international system and were located at Fp1, Fp2, C3, C4, O1, O2, TP9 and TP10, referenced to Cz. For a layout, see Fig A in [S1 Text](#). The dataset lengths varied between 12.9 and 54.9 minutes ( $32.2 \pm 10.0$  minutes, mean  $\pm$  SD). The EEG sampling frequency was 1024 Hz. Apgar scores, to assess the newborn wellbeing, were recorded at 1 and 5 minutes after birth.

### 2.2. Preprocessing and measures estimation

All analyses were performed in Matlab R2022b (The MathWorks, Natick, MA, USA). We first linearly detrended the raw EEG data. Data were then band-pass filtered between 1 and 45 Hz using a finite impulse response (FIR) filter order of 2048 (i.e., twice the sampling rate of the signal). At this point, independent component analysis (ICA) was applied to identify and remove artifacts related to eye movements and cardiac activity. The ICA decomposition was performed using the FastICA algorithm [36] in EEGLAB [37], and components corresponding to physiological artifacts were identified by visual inspection and manually rejected. Besides ICA, data were also manually inspected for noise and artifact. Note that we did not automatically reject bad data (e.g., based on an amplitude or kurtosis threshold), since standard automated artifact rejection procedures would also eliminate bursting activity. Then, and before proceeding with the estimation of neural complexity, we divided the EEG datasets into non-overlapping 10-second windows, resulting in  $N = 10,240$  timepoints per window. EEG sections manually identified as containing artifacts were excluded from complexity calculation.

For each of the non-overlapping windows, we calculated the multiscale entropy (MSE) [38], Lempel-Ziv compressibility (LZ) [39], context tree weighting (CTW) [40,41] as well as a recently introduced estimator called complexity via state-space entropy rate (CSER) [42], which is particularly valued for its temporal resolution, a relevant advantage in our analysis of EEG segments containing only burst or non-burst waveforms. The selection of these entropy measures was guided by the need to include one based on state-space signal reconstruction (MSE), one derived from a compression algorithm (LZ), one based on Markov models (CSER), and a method that combines compression-based and Markov model-based approaches (CTW). LZ, CTW, and CSER are measures of the entropy rate and were implemented using code from a publicly available GitHub repository [43]. For mathematical definitions of each complexity measure, see *Section 2.2.2*.

For each complexity estimator, computed values were averaged across windows within subject. Despite the fact that dividing a dataset into separate windows decreases the number of data points for the measures' calculations, this procedure is more effective in mitigating the influence of noise and artifacts that are common in neurophysiological recordings in newborns. On the other hand, SAT detection was applied to each EEG dataset as a whole, rather than using a windowed approach (see below).

In a further analysis, we divided the datasets into windows 1) with SATs and 2) interburst windows without SATs. Only detected SATs lasting at least 3 seconds were considered as true bursts. Then, we separately calculated our complexity measures for these two periods. Conversely, when windows were longer than 10240 samples (10 seconds), they were divided into non-overlapping windows consisting of 10240 samples.

**2.2.1. SAT detection.** SATs in the EEG were detected over each EEG channel using a nonlinear energy operator algorithm [44]. We then defined proportion-SAT (pSAT) as the proportion of data points detected as SATs over the total duration of the dataset. Consecutive bursts that occurred within 0.5 seconds of each other were merged. An example of a SAT detected in a representative EEG signal is depicted in Fig B in [S1 Text](#). For our analyses, the average pSAT across all channels was taken as a parameter of interest.

**2.2.2. Complexity measures.** We estimated EEG signal complexity using four different complexity measures described earlier: MSE, LZ, CTW, and CSER. The EEG signal was divided into non-overlapping 10 second windows and then z-scored, within each window, prior to estimating each complexity measure for each window that did not contain noise or artifact. The MSE algorithm computes sample entropy (SampEn) [45] at multiple coarse-grained timescales to account for temporal patterns at both short and long scales [46]. SampEn is given by

$$\text{SampEn} = -\ln \left( \frac{\sum_{i=1}^{N-m} n_i^m(r)}{\sum_{i=1}^{N-m} n_i^{m+1}(r)} \right) \quad (1)$$

where  $m$  is the embedding dimension and  $n_i^m(r)$  is the number of vectors  $x^m(t_j)$  which are within a distance  $r$  of  $x^m(t_i)$  without counting instances of  $i=j$  [45]. We used  $m=2$  as the embedding dimension and a time delay of  $t=1$ , consistent with standard applications of SampEn. In addition, we chose  $r=0.15 \sigma$ , where  $\sigma$  is the signal's standard deviation, and we recalculated  $\sigma$  to update this radius for each timescale, thus patching a criticism of the original MSE algorithm [47,48]. We computed SampEn for 20 timescales and derived the corresponding signal frequency at each timescale by dividing the sampling frequency by the scale length. Neural complexity was analyzed for scales between 6–20, as lower coarse grained timescales do not meaningfully alter the signal in light of the bandpass filter already applied during preprocessing. Next, we averaged MSE at the relevant timescales to obtain a single representative value for each participant. Note that in one participant's data, we replaced INF (infinite value) with NaN (not-a-number) values before averaging (MATLAB function: nanmean).

Next, we calculated LZ complexity according to the eponymous compression algorithm [39] following binarization of the EEG signal. In essence, the LZ algorithm proceeds by counting the number of distinct substrings, or "patterns" in a binarized signal, and assigning a higher complexity to signals with more distinct patterns. Specifically, we binarized the EEG using its median value as a threshold; LZ was then normalized by  $T/\log_2(T)$ , where  $T$  is the signal's window length, to yield an entropy rate [49].

In contrast, the CTW algorithm estimates complexity by building a decision tree-based predictor that computes the most likely next state of the signal based on its past states, and assigning low complexity to highly predictable signals. For the CTW calculation, the signal was discretized into  $S = 8$  discrete symbols (i.e., octiles) before being processed by the algorithm. In total, we obtained 32 dependent variables per participant (8 channels x 4 complexity measures).

Complexity via state-space entropy rate (CSER) is similar to CTW in the sense that it involves fitting a predictive model to the signal and estimating complexity from the performance of the predictor. Instead of using a decision tree, CSER uses a state-space model, which models a signal  $x_t$  as being generated by a hidden process  $z_t$ ,

$$z_{t+1} = Az_t + K_{\varepsilon_t} \quad (2)$$

$$x_t = Cz_t + \varepsilon_t \quad (3)$$

The main objects of interest are the  $\varepsilon_t$ , often referred to as *residuals*. Once the model has been fit, CSER is calculated as the entropy of the residuals,

$$\text{CSER} = \frac{1}{2} \log[2\pi e \text{Var}(\varepsilon_t)] \quad (4)$$

For the calculation of CSER, we further downsampled the EEG signal to 128 Hz [42] and estimated the optimal state-space model order by setting the vector autoregressive model order to a maximum of 15. A major motivation for the recent development of CSER was to create a measure of neural complexity that can be spectrally decomposed without a surrogate data test [42]. Thus, to measure signal complexity by EEG frequency, we decomposed CSER into the following frequency bands: delta (1–4 Hz), theta (4–8 Hz), alpha (8–12 Hz), beta (12–30 Hz), gamma (30–45 Hz). Calculation of CSER for frequency bands was conducted on the whole signal, during bursts and during interburst intervals.

Finally, as a supplemental analysis, we explored a much shorter, 1 s window size, using CTW, an entropy rate measure that is well suited for short segments of data [50]. To reduce computation time, 60 windows were chosen at random for each dataset, and CTW was computed within each window from all 8 EEG channels. In case some noisy windows were selected, at least 30 valid windows were retained in each dataset. We then correlated CTW with a continuous measure that increases with bursts, the EEG signal wave envelope. The wave envelope was computed as the instantaneous amplitude of the signal's Hilbert transform smoothed with a 2 s moving average filter and  $\log_{10}$  transformed.

**2.2.3. Analysis of aperiodic components in the EEG signal.** Generally speaking, signals with a strong aperiodic exponent taper off rapidly in power with frequency and are often heavily weighted toward delta activity, whereas signals with a weak aperiodic exponent show a fuller, richer spectrum in which high frequency activity accompanies low frequency activity. Recent work [1] has shown that the aperiodic exponent follows a strong, inverse correlation with complexity in resting EEG from children and adults, as both metrics reflect distinct yet related aspects of signal complexity. Therefore, to further investigate the relationship between pSAT, neural complexity, and the spectral profile of the EEG signal, we calculated the aperiodic exponent of the EEG signals using the FOOOF (Fitting Oscillations and One-Over-F) algorithm [1], which models power spectral density as a combination of aperiodic and periodic components. The aperiodic exponent was calculated to explore its relationship with our complexity measures rather than being considered a primary outcome variable. EEG data were segmented into 10-second windows, and power spectral densities were computed using a wavelet-based time-frequency transformation with a frequency range of 1–45 Hz. The FOOOF model included the following settings: peak width limits between 1 and 10 Hz, maximum number of peaks set at 4, and 'fixed' was selected for the aperiodic mode. For each of the 8 EEG channels, the power spectral density was computed using Morlet wavelets and averaged across time, and FOOOF was applied to extract the aperiodic exponent. The mean aperiodic exponent was calculated across channels and windows for each participant. This value was then used to examine the relationship between the aperiodic component of the signal and neural complexity.

## 2.3. Statistics

Given the multicollinearity of our neural complexity measures, we reduced the dimensionality of our complexity data by computing the average complexity value across all channels for each complexity metric separately. Next, we modeled each channel average using a stepwise regression model with the MATLAB function `stepwiselm`. We selected model predictors using the sum of squares error with default `stepwiselm` parameters. Each linear model started with only an intercept term before considering the addition of the following variables: GA, sex, age at birth (measured in gestational weeks), birth weight (measured in grams), Apgar score (measured approximately 1 minute after birth), and EEG burst percentage. To further understand the pairwise relationships between developmental variables, spectral profile and neural complexity, we then calculated the correlation matrix between GA, pSAT, aperiodic exponent, birth weight, and the Apgar score at time 1 and our four complexity measures (LZ, MSE, CTW, and CSER), computed for each individual channel on the whole signal. Using the MATLAB '`corrcoef`' function we computed the Pearson correlation coefficients with an alpha level of 0.05 for each correlation. To explore potential differences in complexity measures between burst and interburst periods, we computed the channel-averaged complexity estimates for each window type separately. These averaged values were then

entered into a stepwise linear regression model, following the same procedure as described previously, to identify significant predictors of neural complexity across bursts and interburst periods. Then, to compare entropy measures between bursts and interburst periods, we compared the channel-average complexity estimates using a paired sample t-test.

Next, we computed the correlation matrix between developmental variables and channel-averaged CSER across different frequency bands, calculated separately for the whole signal, bursts, and interburst periods. As previously done, we used the 'corrcoef' function to calculate Pearson correlation coefficients for each relationship, applying an alpha level of 0.05.

Finally, we investigated possible mediation relationships in our data using the MATLAB mediation toolbox by Wager and colleagues [51,52]. Specifically, we investigated two basic mediation models. In the first model a relationship between GA and complexity is mediated by pSAT; in other words, we asked whether maturation drives changes in EEG burst activity, which in turn drives changes in complexity. In the second model, a relationship between pSAT and complexity is mediated by the aperiodic exponent; in other words, we asked whether bursting drives changes in the EEG 1/f background slope, which in turn drives changes in complexity. Each model was run for each complexity measure computed from the whole signal, bursts, and interburst periods.

To correct for multiple testing, we applied the false discovery rate (FDR) correction method by Benjamini and Hochberg [53]. This was done separately for 1) the main tests reported in Table 2, 2) correlations displayed in Fig C and Fig D in S1 Text, 3) the band-limited CSER results displayed in Fig E in S1 Text, and 4) the mediation model results reported in Table A in S1 Text.

## 2.4. Burst simulation

To investigate whether signal complexity increases as a necessary consequence of burst waveforms, we simulated EEG signals using artificial 1/f noise time series (MATLAB function: dsp.ColoredNoise). The number of simulated signals was chosen to match the number of infants with usable data, and the simulated signal length was chosen to match the minimum data length from our infant EEG sample. Bursts were randomly added to simulated signals with a burst duration of 2 – 10 seconds, and an interburst interval of 3 – 30 seconds.

## 3. Results

### 3.1. Infants

Of the 32 preterm infants recruited, 28 were eligible for analyses after preprocessing and data quality assessment; 4 infants were excluded either due to excessive movement or because at least one electrode detached. The characteristics for included participants are available in Table 1. Age distribution of our sample is displayed in Fig A in S1 Text.

### 3.2. Neural complexity in the whole EEG signal

Our first step was to reduce the dimensionality of our data by calculating the average complexity value across channels for each measure separately; this decision was supported by the low spatial variance of complexity measures, illustrated by largely homogeneous topographic scalp plots (Fig F-H in S1 Text). Following stepwise regression, which in all cases included an intercept term, we found that channel-averaged MSE was higher in females than in males ( $t = -3.8$ ,  $P_{\text{FDR}} = 0.0012$ , Fig 1A). Next, LZ significantly decreased with pSAT ( $t = -5.2$ ,  $P_{\text{FDR}} = 0.00011$ , Fig 1B). CSER was positively related to GA ( $t = 2.2$ ,  $P_{\text{FDR}} = 0.037$ , Fig 1C) and negatively to pSAT ( $t = -3.1$ ,  $P_{\text{FDR}} = 0.0057$ , Fig 1C). Finally, CTW also negatively related to pSAT ( $t = -4.5$ ,  $P_{\text{FDR}} = 0.00045$ , Fig 1D). Next, we computed the correlation matrix between complexity measures, calculated for individual channels, and developmental variables. This showed strong correlations between complexity measures, as previously reported (for example [28]), and largely consistent associations between complexity and developmental variables (see Fig C in S1 Text). Additionally, the aperiodic exponent was negatively correlated with all complexity estimates, in agreement with previous work by others [1].

Finally, to resolve spectral information for signal complexity, we calculated CSER from the whole EEG signal according to a spectral decomposition for delta (1–4 Hz), theta (4–8 Hz), alpha (8–12 Hz), beta (12–30 Hz), gamma (30–45 Hz) frequency bands. The correlation matrix between spectrally decomposed CSER values and developmental variables is presented as

**Table 1. Participant characteristics.**

Variable	Mean $\pm$ SD	Range
Age at birth (weeks)	29.2 $\pm$ 2.0	25–33
Age at recording (weeks)	30.9 $\pm$ 1.9	27–35
Weight at birth (g)	1254.4 $\pm$ 324.5	750–1950
Weight at recording (g)	1388.6 $\pm$ 347.4	900–2180
Apgar 1	7.9 $\pm$ 2.0	2–10
Apgar 5	9.1 $\pm$ 1.3	4–10
pSAT	35.5 $\pm$ 14.0	4.9–66.2
Aperiodic exponent	2.2 $\pm$ 0.2	1.8–2.5
Recording length (min)	32.2 $\pm$ 10.0	12.9–54.9

<https://doi.org/10.1371/journal.pcsy.0000056.t001>

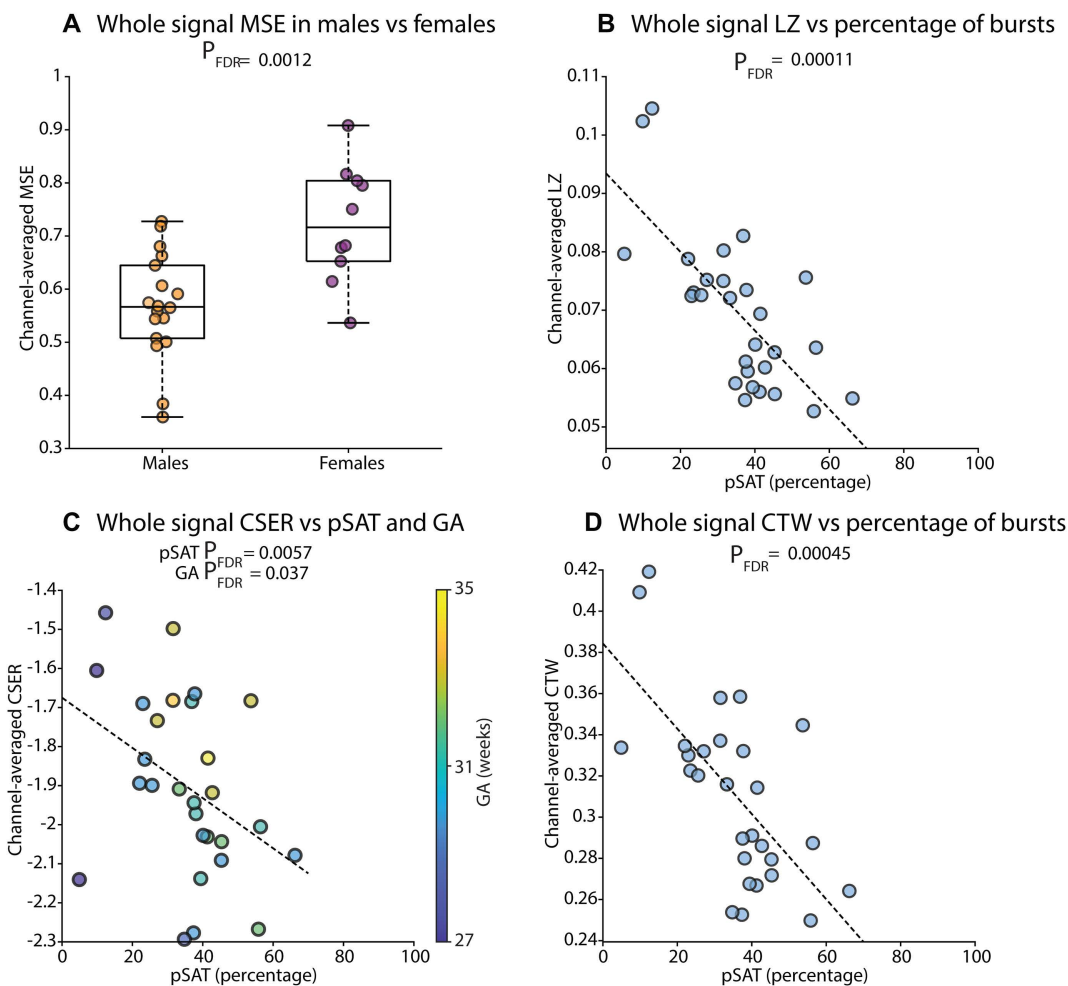


**Fig 1. Predictive variables for channel-averaged complexity measures obtained from the whole signal.** For P-values and test statistics, see [Table 2](#).

<https://doi.org/10.1371/journal.pcsy.0000056.g001>

a heatmap in Fig D in [S1 Text](#). For CSER results yielded from each frequency (Fig I in [S1 Text](#)), we fit the same model as previously selected by the stepwise procedure for broadband CSER with GA and pSAT as predictors. We found that pSAT significantly predicted CSER in each of the five frequency bands, but GA only significantly predicted CSER in the alpha and

beta bands (Fig E, panels a-e, in [S1 Text](#)). Finally, t-tests revealed that CSER is consistently greater during EEG bursts compared with IBIs, regardless of the frequency band (Fig E, panels f-j, in [S1 Text](#), Table A in [S1 Text](#)).

### 3.3. Neural complexity during burst and interburst periods

Following stepwise regression, we found that, during periods of burst, channel-averaged MSE was positively related to GA ( $t=4.0$ ,  $P_{FDR}=0.00081$ , [Fig 2A](#)); CSER positively related to pSAT ( $t=4.1$ ,  $P_{FDR}=0.00071$ , [Fig 2B](#)) and was higher in males compared to females ( $t=2.2$ ,  $P_{FDR}=0.037$ , [Fig 2B](#)). CTW was also positively related to GA ( $t=2.7$ ,  $P_{FDR}=0.011$ , [Fig 2C](#)).

When considering interburst periods, MSE was lower in males compared to females ( $t=-2.8$ ,  $P_{FDR}=0.012$ , [Fig 3A](#)). In addition, LZ ( $t=-4.9$ ,  $P_{FDR}=0.00021$ , [Fig 3B](#)) and CTW ( $t=-4.2$ ,  $P_{FDR}=0.00055$ , [Fig 3D](#)) negatively related to pSAT. CSER, on the contrary, positively related to pSAT ( $t=3.6$ ,  $P_{FDR}=0.0020$ , [Fig 3C](#)).

### 3.4. Causal mediation analysis

Based on the foregoing, pSAT would appear to be the main driver of between-subjects variance in complexity. However, it is known that the continuity of EEG burst patterns changes with GA in preterm infants [\[54\]](#), and indeed, our data showed a strong correlation between GA and pSAT ( $r=0.51$ ,  $P_{FDR}=0.008$ ; see Fig C in [S1 Text](#)). Therefore, it is plausible that pSAT actually mediates relationships between GA and complexity. Furthermore, it is also plausible that EEG bursts alter the spectral 1/f background of the EEG signal, an effect which might in turn drive complexity changes. While pSAT was not significantly correlated ( $r=0.28$ ,  $P_{FDR}>0.05$ ) with the aperiodic exponent—a measure of the steepness of the 1/f background—we nonetheless decided out of caution to test models wherein the aperiodic exponent mediates a relationship between pSAT and complexity.

The mediation analysis yielded a trend-level effect ( $P_{FDR}=0.08$ ) for pSAT as a mediator between GA and all complexity measures computed from the whole signal or the interburst signal, as well as CSER computed from the burst signal (see Table B in [S1 Text](#)). On the other hand, the effect for the aperiodic exponent as a mediator between pSAT and complexity was neither significant nor trending for any complexity measure, regardless of whether it was computed from the whole signal, the burst signal, or the interburst signal.

### 3.5. Differences in neural complexity between burst and interburst periods

Our final goal was to compare complexity measures between bursts and interburst periods. To this end, we compared the channel-average complexity estimates between the two types of windows using a paired sample t-test. Each complexity measure was significantly different between burst and interburst segments. Specifically, MSE ( $t=-4.3$ ,  $P_{FDR}=0.00051$ , [Fig 4A](#)),

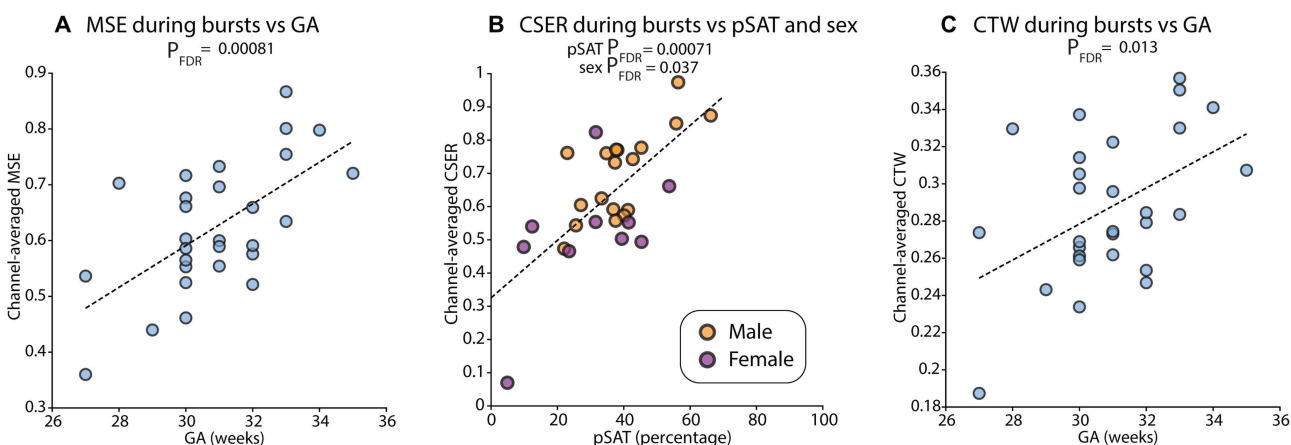


**Fig 2. Complexity measures during bursts.** For P-values and test statistics, see [Table 2](#).

<https://doi.org/10.1371/journal.pcsy.0000056.g002>

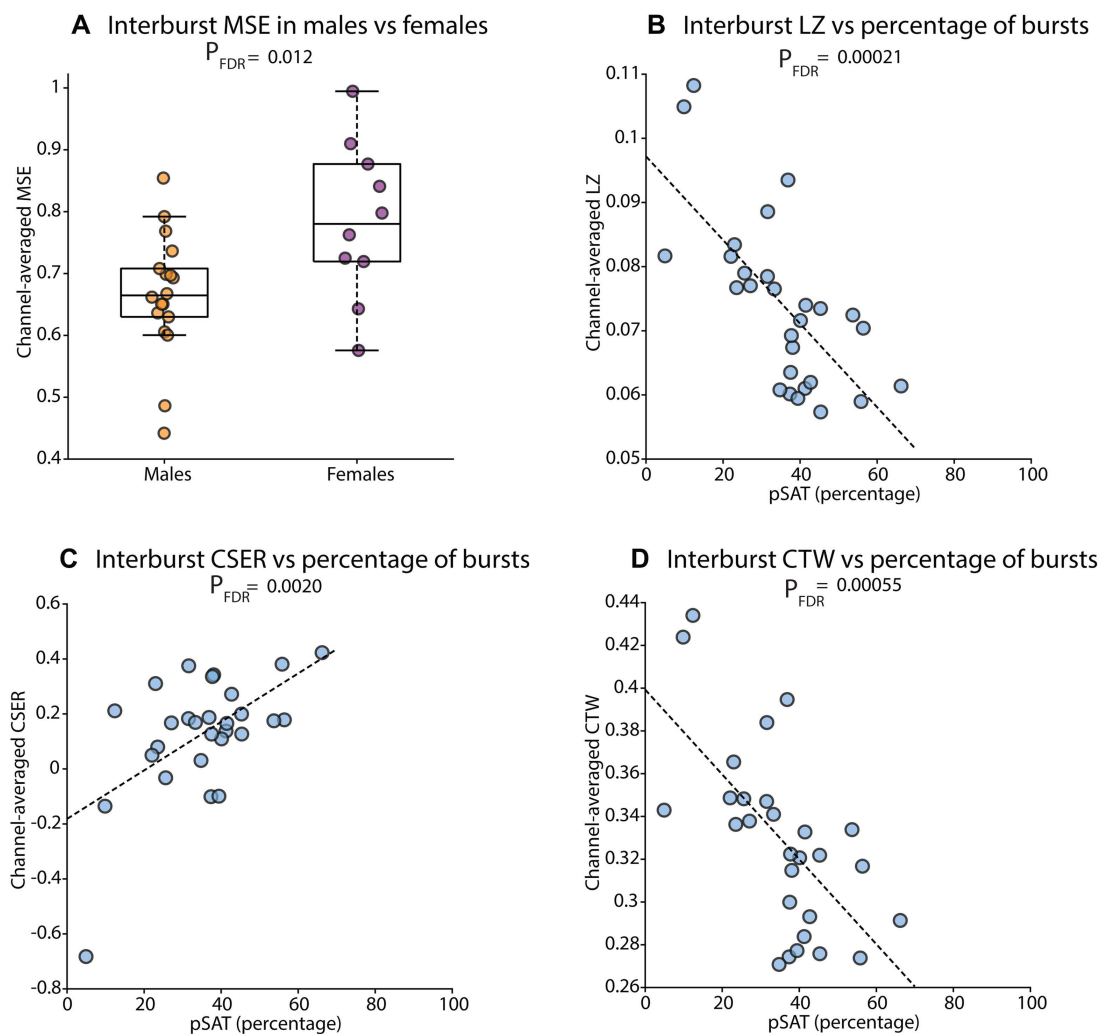


**Fig 3. Complexity measures during interburst periods (IBIs).** For P-values and test statistics, see [Table 2](#).

<https://doi.org/10.1371/journal.pcsy.0000056.g003>

LZ ( $t = -4.3$ ,  $P_{FDR} = 0.00051$ , [Fig 4B](#)), and CTW ( $t = -5.2$ ,  $P_{FDR} = 0.00011$ , [Fig 4D](#)) were lower during bursts compared to interburst periods. On the contrary, CSER was higher during bursts compared to interburst periods ( $t = 19.7$ ,  $P_{FDR} = 2.5E-16$ , [Fig 4C](#)). To confirm that an overall inverse relationship between neural complexity and EEG bursts remained even when neural complexity was examined with finer temporal resolution, we used CTW – which is preferable for short data segments [50] – computed the CTW entropy rate in 1 s windows, and correlated this measure with the EEG signal's log-scaled wave envelope, which increases during bursts (Fig J in [S1 Text](#)). This correlation was consistently negative, with a median Pearson coefficient across datasets of  $r = -0.63$  (Fig K in [S1 Text](#)).

### 3.6. Simulated bursts do not recapitulate EEG results

To address the possibility that correlations between pSAT and signal complexity are an inevitable consequence of burst waveforms, we simulated  $n = 28$  1/f noise signals with a duration of 13 minutes, i.e., approximately the same duration as the shortest EEG recording in our dataset. Artificial signals were generated using a spectral exponent of  $\alpha = 2$ , or approximately the average aperiodic exponent observed in our EEG data. No significant or trend-level correlations were

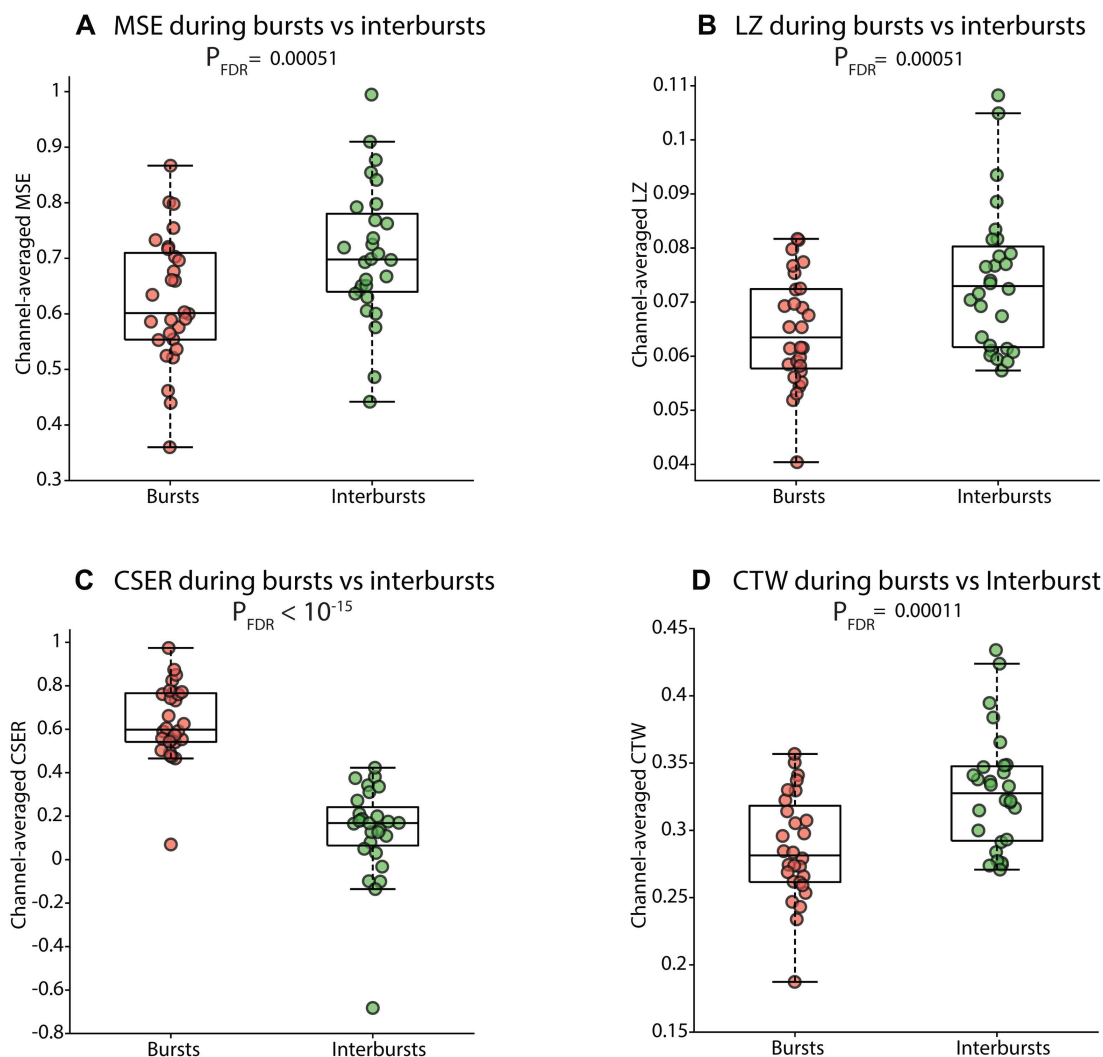


**Fig 4. Comparisons of complexity between burst and interburst periods.** For P-values and test statistics, see [Table 2](#).

<https://doi.org/10.1371/journal.pcsy.0000056.g004>

observed between complexity measures and pSAT in artificial signals, even without correcting for multiple testing (Fig L in [S1 Text](#)).

#### 4. Discussion

In this study, we investigated the complexity of neural signals as it relates to developmental variables by using complexity estimation algorithms applied to spontaneous EEG recordings from preterm infants. We sought to understand the evolution of neural complexity during the neonatal period in relation to GA (gestational age), biological sex, and periods of cortical burst or interburst activity. Specifically, and consistently with prior work from our group [28], we measured neural complexity as the EEG signal entropy (MSE) or entropy rate (LZ, CTW, and CSER). While other rigorous definitions of complexity have been proposed [55] that aim to quantify the structure of a signal, here we use the term complexity as a synonym for signal diversity, a meaningful quantity that scales across a wide range of contexts with the brain's capacity for information processing and level of consciousness [6,7,42,56–58]. Although quantifying signal complexity or diversity is challenging [55], prior work [28,59] has noted that many estimators of functional brain signal entropy or entropy rate

seem to capture a common underlying property of the signal, which is often conceptualized as “complexity as entropy” or “statistical complexity” [60]. Here, too, we found strong correlations in our data among estimators of neural entropy or entropy rate (see Fig C in [S1 Text](#)), suggesting a common denominator which we refer to as neural complexity. Our results demonstrate that neural complexity is predicted by developmental variables and tracks developmentally meaningful processes, including the maturation of signal dynamics which become more continuous with age. In particular, correlations were common between neural complexity and pSAT – the proportion of time during which bursts were observed in the signal – and this finding was not reproduced in a simulation using artificial 1/f noise signals and square wave bursts, suggesting that our results are not merely an inevitable consequence of the manner in which entropy or entropy rate estimator algorithms respond to burst waveforms.

#### 4.1. The evolution of neural complexity is driven by changes in signal continuity

Neonatal cortical dynamics are characterized, particularly in preterm infants, by discontinuous patterns of bursting activity, on the one hand, and quiescent activity, on the other hand. As the thalamocortical system matures, the efficacy of the thalamus to drive the cortex increases, resulting in a more continuous pattern of bursting activity [54,61]. In premature newborns, bursts of cortical activity lead to interactions at the level of a network comprising thalamic afferents, the horizontal nexus of the cortical subplate, and the cortical plate. Bursts of activity similar to that recorded with EEG are also found in recordings from subplate postmortem brain slices from human fetuses at 21 weeks of gestation [62]. This suggests that subplate neurons play a significant role in generating brain activity characterized by bursts.

Past studies [21,22,29] have observed an increase in neural complexity during the neonatal period without connecting these changes to the fundamental dynamics of cortical signals (bursting versus quiescent). Here, we found strong evidence to support the hypothesis that the information-rich signal fluctuations which occur during burst periods may drive changes in neural complexity as estimated from several algorithms we employed (MSE, LZ, CTW, and CSER). When considering the EEG signal as a whole (i.e., without separately analyzing bursts or interburst periods), neural complexity measured by LZ, CTW and CSER significantly decreases in a linear fashion as the proportion of bursts (pSAT) increases ([Fig 1B–D](#)). Given the organized and stereotyped spatiotemporal characteristics of bursts, these results were largely expected.

Notably, the foregoing pattern persisted even when interburst intervals (IBIs) were analyzed separately, with both LZ and CTW values during IBIs decreasing as bursts occurred more often ([Fig 3B, D](#)). These correlations were unexpected, given that IBIs, by definition, exclude bursting activity. It is possible that as the brain matures, burst waveforms grow more complex – a conclusion supported by complexity estimates (MSE and CTW) during bursts which positively correlated with gestational age ([Fig 2A, C](#)) – at the expense of IBIs, which grow proportionally less complex. However, the decrease in complexity during IBIs was not observed with all complexity estimators: in contrast to LZ and CTW, CSER increased with the proportion of bursts ([Fig 3C](#)), suggesting that it is sensitive to different signal properties.

As mentioned above, when burst periods were considered in isolation, both MSE and CTW increased with gestational age, thus aligning with previous literature [21,22,29]. However, these previous studies have included infants across a broader range of gestational ages, generally extending to term-equivalent age. In these infants, the EEG signal is dominated almost entirely by bursting activity, which may drive the overall increase in neural complexity with age. In contrast, infants in our cohort are younger and exhibit a more discontinuous pattern with relatively sparse bursting. As a result, developmental increases in complexity seen in our data were primarily detectable during bursts themselves, while the overall EEG signal, still heavily shaped by IBIs, shows a less pronounced age-related effect. These findings suggest that with advancing gestational age, not only does the repetition frequency of bursting increase, but the bursts themselves also become more structured and information-rich, reflecting enhanced neural activity.

Comparing complexity measures between burst periods and IBIs further supported and extended the findings of the current work. Across most algorithms (MSE, LZ, and CTW), complexity was consistently lower during bursts than during IBIs. This likely reflects the structured and stereotyped nature of bursts, which stand in contrast to the more variable and

less organized activity typical of IBIs. Once again, CSER demonstrated an opposite trend, with higher complexity values during bursts than IBIs. This divergence highlights important differences in how these algorithms seem to capture neural signal properties, e.g., perhaps bursts have a strong non-stationary component not captured by CSER. Further work is necessary to determine why CSER diverges from other entropy rate measures.

#### 4.2. Do bursts mediate a relationship between gestational age and neural complexity?

An important question raised by our results is whether the proportion of bursts (pSAT) mediates a relationship between gestational age and neural complexity. Gestational age and pSAT are strongly correlated (Fig C in [S1 Text](#)), and of the two variables, gestational age is fundamentally independent, i.e., it is only caused by the passage of time and thus positions itself as the explanatory variable. Furthermore, gestational age was measured in weeks and many subjects shared the same gestational age as measured with this relatively coarse level of precision. By comparison, pSAT was measured with much higher precision and, thus, may have been favored as an explanatory variable by the stepwise regression procedure as it carried more information.

While a mediation model is intuitive, we did not find significant evidence for pSAT as a mediator variable. Nonetheless, all models run using complexity computed from either the whole signal or the interburst periods showed a trend-level mediation effect (Table B in [S1 Text](#)). Although we performed frequentist statistics, an informal Bayesian approach may also be helpful: given neurodevelopmental processes which increase pSAT with age [54], we view mediation as both a likely and useful framework for conceptualizing the dependencies between gestational age, pSAT, and neural complexity. In the broader context of previous work [21,63], findings of increasing neural complexity with gestational age in preterm infants are likely explained by the mediating influence of transitions from discontinuous to continuous signal dynamics with age. Finally, while auditory-evoked fetal recordings have shown the opposite trajectory – decreasing neural complexity with gestational age [28] – this could be explained by the fact that trial-averaged evoked responses lack the dimension of pSAT which drives age-related complexity increases in spontaneous data.

#### 4.3. Does EEG complexity depend on spectral properties?

Finally, a further question remains whether spectral power changes mediate the relationship between pSAT and neural complexity. Thus, we tested the aperiodic exponent (i.e., the steepness of the  $1/f$  EEG background) as a mediator derived from the power spectrum; this variable follows a strong, inverse correlation with EEG signal complexity both in previous work [1] and our own results (Fig C in [S1 Text](#)). We found no significant or even trend-level mediation effect when pSAT was treated as the independent variable and complexity measures were treated as the dependent variable. While this null result supports our focus on neural complexity rather than spectral properties, it remains possible that oscillatory power at a given frequency might partially mediate the relationship between pSAT and complexity. Excluding this possibility would require a more exhaustive search beyond the scope of the current study. However, to partially address the role of each EEG frequency band in our complexity results, we utilized a spectral decomposition of the entropy rate using CSER, whose development was partially motivated by the need for a spectral decomposition of the entropy rate, which cannot be obtained from the other metrics in a principled manner [42]. The spectral decomposition of CSER (Fig E in [S1 Text](#)) revealed largely consistent results across frequency bands, though the strongest correlation with pSAT occurred in the delta band, suggesting that bursts alter neural complexity at slow timescales. On the other hand, CSER only correlated with gestational age at faster frequencies – specifically, alpha and beta – suggesting that pSAT does not simply mediate a relationship between gestational age and the neural entropy rate.

#### 4.4. Neural complexity is influenced by sex

A puzzling recent finding is that neural complexity is influenced by fetal sex in auditory-evoked MEG signals [28] recorded between 25 and 40 gestational weeks, with female fetuses exhibiting greater signal complexity, especially later in gestation. While preterm infants are not perfect models of gestational age-equivalent fetuses [64], there is sufficient similarity

that we hypothesized that we would recapitulate the above finding in spontaneous EEG recorded from preterm infants. In fact, we found three instances in which sex indeed predicted neural complexity (Figs 1–3, Table 2). These differences were observed on MSE values computed both on the whole signal and during IBIs, where male infants showed lower brain complexity compared to females. In contrast, CSER computed specifically during burst periods revealed the opposite pattern, with males showing higher complexity than females. Overall, our findings largely corroborate prior work [28], where MSE was computed from MEG according to the Xie et al. algorithm [65] and several other neural complexity measures were greater in female versus male fetuses; note that this study did not examine CSER, which was introduced in work published only a few months prior [42].

Nonetheless, the neurobiological reason for an influence of sex on neural complexity during the perinatal period remains mysterious. Addressing this unsolved problem might be relevant toward efforts to develop neural complexity as a biomarker of early risk for neurodevelopmental disorders, which are often more common in boys than in girls. For instance, autism spectrum disorder is diagnosed approximately four times more often in boys than in girls [66] and less extreme gender ratios are also skewed toward boys in the diagnosis of attention deficit hyperactivity disorder [67] and Tourette syndrome [68], as well as childhood obsessive-compulsive disorder [69]. Moreover, neural complexity recorded with EEG at as early as 3 months of age is predictive of autism diagnosis in a cohort with familial risk [14]. Future work should explore whether neural complexity recorded during the perinatal period, either using fetal MEG or infant EEG, can predict autism diagnosis even earlier using a similar study design that recruits pregnancies with high familial risk.

#### 4.5. Limitations

Several limitations of our study should be noted, all stemming from the clinical context in which data were obtained. Firstly, we could not control the sleep states of the preterm infants who gave data in a clinical setting, and thus, EEG recordings likely contain a mixture of sleep and wakefulness. While this somewhat hinders the interpretation of our results, the same issue also affects recordings of fetal MEG data in research settings [28,34], and our data yielded significant results that were useful toward testing our hypotheses nonetheless. Secondly, our sample size (n = 28 infants with usable data) was modest, and we may have been underpowered to detect statistical relationships with small effect sizes. Furthermore, only

**Table 2. Predictive variables and complexity measures computed on the whole signal, during bursts, or during interburst periods.**

Complexity measure	Predictor	T-stat	P <sub>FDR</sub>
Whole signal MSE	Sex	-3.8	0.0012
Whole signal LZ	Bursts	-5.2	0.00011
Whole signal CSER	GA	2.2	0.037
Whole signal CSER	Bursts	-3.1	0.0057
Whole signal CTW	Bursts	-4.5	0.00045
MSE during bursts	GA	4.0	0.00081
CSER during bursts	Bursts	4.1	0.00071
CSER during bursts	Sex	2.2	0.037
CTW during bursts	GA	2.7	0.013
MSE during interburst	Sex	-2.8	0.012
LZ during interburst	Bursts	-4.9	0.00021
CSER during interburst	Bursts	3.6	0.0020
CTW during interburst	Bursts	-4.2	0.00055
MSE in bursts vs. interburst	Difference	-4.3	0.00051
LZ in bursts vs. interburst	Difference	-4.3	0.00051
CSER in bursts vs. interburst	Difference	19.7	2.5E-16
CTW in bursts vs. interburst	Difference	-5.2	0.00011

<https://doi.org/10.1371/journal.pcsy.0000056.t002>

8 channels were recorded from each infant, and thus, we were not strongly positioned to examine EEG spatial dynamics or spatial topographies. However, given that we did not have an anatomical hypothesis, we did not consider this to be a major limitation. Finally, the GA range of our sample reflects the limitations of collecting data in a clinical setting, where extremely premature infants are underrepresented.

## 5. Conclusions

We showed that neural complexity in preterm infants is influenced by developmental variables, including the continuity of neural signals, gestational age, and sex. In particular, we found that CSER, a newer algorithm for measuring neural complexity, behaves differently from older algorithms in interesting and relevant ways. While we focused on the temporal dimension of neural complexity, parallel and independent work by others is currently investigating the spatial dimension of neural complexity in preterm infants using high density EEG with promising results [70]. We anticipate that both lines of work may converge in the near future to demonstrate the general importance of neural complexity as a potential predictive biomarker of developmental outcomes in preterm infants [71]. In light of this, future studies should investigate long term trajectories of neural complexity into toddlerhood, e.g., as it may relate to atypical development. Finally, because EEG burst dynamics are not exclusive to infancy, but also appear in adults during states of greatly attenuated consciousness such as disorders of consciousness or deep anesthesia [72], our results may also have implications for explaining why neural complexity is also reduced during the absence of consciousness [56]. Future work should test whether our results generalize to burst patterns recorded in adult EEG during states of unconsciousness, e.g., by demonstrating that increasing burst tendency drives reductions in neural complexity.

## Supporting information

### S1 Text. Supporting information.

(PDF)

## Author contributions

**Conceptualization:** Lorenzo Semeia, Joel Frohlich.

**Data curation:** Lorenzo Semeia, Dimitrios Metaxas, Mina Nourhashemi, Mahdi Mahmoudzadeh, Joel Frohlich.

**Formal analysis:** Lorenzo Semeia, Joel Frohlich.

**Funding acquisition:** Dimitrios Metaxas, Andreas L. Birkenfeld, Hubert Preissl, Fabrice Wallois.

**Investigation:** Mina Nourhashemi, Mahdi Mahmoudzadeh, Fabrice Wallois.

**Methodology:** Lorenzo Semeia, Pedro A. M. Mediano, Joel Frohlich.

**Project administration:** Hubert Preissl, Fabrice Wallois.

**Resources:** Mina Nourhashemi, Mahdi Mahmoudzadeh, Fabrice Wallois.

**Software:** Lorenzo Semeia, Amer Zaylaa, Katrin Sippel, Pedro A. M. Mediano.

**Supervision:** Andreas L. Birkenfeld, Hubert Preissl, Joel Frohlich.

**Validation:** Dimitrios Metaxas.

**Visualization:** Lorenzo Semeia, Joel Frohlich.

**Writing – original draft:** Lorenzo Semeia, Joel Frohlich.

**Writing – review & editing:** Lorenzo Semeia, Amer Zaylaa, Dimitrios Metaxas, Mina Nourhashemi, Mahdi Mahmoudzadeh, Andreas L. Birkenfeld, Katrin Sippel, Pedro A. M. Mediano, Hubert Preissl, Fabrice Wallois, Joel Frohlich.

## References

1. Donoghue T, Hammonds R, Lybrand E, Washcke L, Gao R, Voytek B. Evaluating and comparing measures of aperiodic neural activity. *bioRxiv*. 2024:2024.09.15.613114. <https://doi.org/10.1101/2024.09.15.613114> PMID: 39314334
2. Lau ZJ, Pham T, Chen SHA, Makowski D. Brain entropy, fractal dimensions and predictability: a review of complexity measures for EEG in healthy and neuropsychiatric populations. *Eur J Neurosci*. 2022;56(7):5047–69. <https://doi.org/10.1111/ejn.15800> PMID: 35985344
3. Stam CJ. Nonlinear dynamical analysis of EEG and MEG: review of an emerging field. *Clin Neurophysiol*. 2005;116(10):2266–301. <https://doi.org/10.1016/j.clinph.2005.06.011> PMID: 16115797
4. Lutzenberger W, Birbaumer N, Flor H, Rockstroh B, Elbert T. Dimensional analysis of the human EEG and intelligence. *Neurosci Lett*. 1992;143(1–2):10–4. [https://doi.org/10.1016/0304-3940\(92\)90221-r](https://doi.org/10.1016/0304-3940(92)90221-r) PMID: 1436649
5. Lutzenberger W, Flor H, Birbaumer N. Enhanced dimensional complexity of the EEG during memory for personal pain in chronic pain patients. *Neurosci Lett*. 1997;226(3):167–70. [https://doi.org/10.1016/s0304-3940\(97\)00268-1](https://doi.org/10.1016/s0304-3940(97)00268-1) PMID: 9175593
6. Mediano PAM, Ikkala A, Kievit RA, Jagannathan SR, Varley TF, Stamatakis EA, et al. Fluctuations in neural complexity during wakefulness relate to conscious level and cognition. Cold Spring Harbor Laboratory; 2021. <https://doi.org/10.1101/2021.09.23.461002>
7. Stolp L, Mandke KN, Mediano PA, Gellersen HM, Swartz A, Rudzka K, et al. Informational complexity as a neural marker of cognitive reserve. *bioRxiv*. 2025 Feb 14;2025–02. <https://doi.org/10.1101/2025.02.13.638084>
8. Müller V, Lutzenberger W, Pulvermüller F, Mohr B, Birbaumer N. Investigation of brain dynamics in Parkinson's disease by methods derived from nonlinear dynamics. *Exp Brain Res*. 2001;137(1):103–10. <https://doi.org/10.1007/s002210000638> PMID: 11310163
9. Acharya UR, Fujita H, Sudarshan VK, Bhat S, Koh JEW. Application of entropies for automated diagnosis of epilepsy using EEG signals: a review. *Knowl Based Syst*. 2015;88:85–96. <https://doi.org/10.1016/j.knsys.2015.08.004>
10. Liu Q, Chen Y-F, Fan S-Z, Abbod MF, Shieh J-S. EEG signals analysis using multiscale entropy for depth of anesthesia monitoring during surgery through artificial neural networks. *Comput Math Methods Med*. 2015;2015:232381. <https://doi.org/10.1155/2015/232381> PMID: 26491464
11. Sun J, Wang B, Niu Y, Tan Y, Fan C, Zhang N, et al. Complexity analysis of EEG, MEG, and fMRI in mild cognitive impairment and Alzheimer's disease: a review. *Entropy*. 2020;22(2):239. <https://doi.org/10.3390/e22020239> PMID: 33286013
12. Anokhin AP, Lutzenberger W, Nikolaev A, Birbaumer N. Complexity of electrocortical dynamics in children: developmental aspects. *Dev Psychobiol*. 2000;36(1):9–22. [https://doi.org/10.1002/\(sici\)1098-2302\(200001\)36:1<9::aid-dev2>3.0.co;2-5](https://doi.org/10.1002/(sici)1098-2302(200001)36:1<9::aid-dev2>3.0.co;2-5)
13. Hadoush H, Alafeef M, Abdulhay E. Brain complexity in children with mild and severe autism spectrum disorders: analysis of multiscale entropy in EEG. *Brain Topogr*. 2019;32(5):914–21. <https://doi.org/10.1007/s10548-019-00711-1> PMID: 31006838
14. Bosl WJ, Tager-Flusberg H, Nelson CA. EEG analytics for early detection of autism spectrum disorder: a data-driven approach. *Sci Rep*. 2018;8(1):6828. <https://doi.org/10.1038/s41598-018-24318-x> PMID: 29717196
15. Bosl W, Tierney A, Tager-Flusberg H, Nelson C. EEG complexity as a biomarker for autism spectrum disorder risk. *BMC Med*. 2011;9:18. <https://doi.org/10.1186/1741-7015-9-18> PMID: 21342500
16. Blencowe H, Cousens S, Oestergaard MZ, Chou D, Moller A-B, Narwal R, et al. National, regional, and worldwide estimates of preterm birth rates in the year 2010 with time trends since 1990 for selected countries: a systematic analysis and implications. *Lancet*. 2012;379(9832):2162–72. [https://doi.org/10.1016/S0140-6736\(12\)60820-4](https://doi.org/10.1016/S0140-6736(12)60820-4) PMID: 22682464
17. Saigal S, Doyle LW. An overview of mortality and sequelae of preterm birth from infancy to adulthood. *Lancet*. 2008;371(9608):261–9. [https://doi.org/10.1016/S0140-6736\(08\)60136-1](https://doi.org/10.1016/S0140-6736(08)60136-1) PMID: 18207020
18. Johnson S, Hollis C, Kochhar P, Hennessy E, Wolke D, Marlow N. Psychiatric disorders in extremely preterm children: longitudinal finding at age 11 years in the EPICure study. *J Am Acad Child Adolesc Psychiatry*. 2010;49(5):453–463.e1. <https://doi.org/10.1016/j.jaac.2010.02.002>
19. Nosarti C, Reichenberg A, Murray RM, Cnattingius S, Lambe MP, Yin L, et al. Preterm birth and psychiatric disorders in young adult life. *Arch Gen Psychiatry*. 2012;69(6):E1–8. <https://doi.org/10.1001/archgenpsychiatry.2011.1374> PMID: 22660967
20. El-Dib M, Abend NS, Austin T, Boylan G, Chock V, Cilio MR, et al. Neuromonitoring in neonatal critical care part II: extremely premature infants and critically ill neonates. *Pediatr Res*. 2023;94(1):55–63. <https://doi.org/10.1038/s41390-022-02392-2> PMID: 36434203
21. De Wel O, Lavanga M, Dorado A, Jansen K, Dereymaeker A, Naulaers G, et al. Complexity analysis of neonatal EEG using multiscale entropy: applications in brain maturation and sleep stage classification. *Entropy*. 2017;19(10):516. <https://doi.org/10.3390/e19100516>
22. Isler JR, Stark RI, Grieve PG, Welch MG, Myers MM. Integrated information in the EEG of preterm infants increases with family nurture intervention, age, and conscious state. *PLoS One*. 2018;13(10):e0206237. <https://doi.org/10.1371/journal.pone.0206237> PMID: 30356312
23. Janjarasjitt S, Scher MS, Loparo KA. Nonlinear dynamical analysis of the neonatal EEG time series: the relationship between neurodevelopment and complexity. *Clin Neurophysiol*. 2008;119(4):822–36. <https://doi.org/10.1016/j.clinph.2007.11.012> PMID: 18203659
24. Scher MS, Waisanen H, Loparo K, Johnson MW. Prediction of neonatal state and maturational change using dimensional analysis. *J Clin Neurophysiol*. 2005 Jun 1;22(3):159–65.
25. Kaffashi F, Scher MS, Ludington-Hoe SM, Loparo KA. An analysis of the kangaroo care intervention using neonatal EEG complexity: a preliminary study. *Clin Neurophysiol*. 2013;124(2):238–46. <https://doi.org/10.1016/j.clinph.2012.06.021> PMID: 22959415

26. Rajagopalan V, Scott J, Habas PA, Kim K, Corbett-Detig J, Rousseau F, et al. Local tissue growth patterns underlying normal fetal human brain gyrification quantified in utero. *J Neurosci*. 2011;31(8):2878–87. <https://doi.org/10.1523/JNEUROSCI.5458-10.2011> PMID: [21414909](https://pubmed.ncbi.nlm.nih.gov/21414909/)
27. van Noordt S, Willoughby T. Cortical maturation from childhood to adolescence is reflected in resting state EEG signal complexity. *Dev Cogn Neurosci*. 2021;48:100945. <https://doi.org/10.1016/j.dcn.2021.100945> PMID: [33831821](https://pubmed.ncbi.nlm.nih.gov/33831821/)
28. Frohlich J, Moser J, Sippel K, Mediano PAM, Preissl H, Gharabaghi A. Sex differences in prenatal development of neural complexity in the human brain. *Nat Mental Health*. 2024;2(4):401–16. <https://doi.org/10.1038/s44220-024-00206-4>
29. Schmidt K, Kott M, Müller T, Schubert H, Schwab M. Developmental changes in the complexity of the electrocortical activity in foetal sheep. *J Physiol Paris*. 2000;94(5–6):435–43. [https://doi.org/10.1016/s0928-4257\(00\)01087-1](https://doi.org/10.1016/s0928-4257(00)01087-1) PMID: [11165911](https://pubmed.ncbi.nlm.nih.gov/11165911/)
30. Ackman JB, Burbridge TJ, Crair MC. Retinal waves coordinate patterned activity throughout the developing visual system. *Nature*. 2012;490(7419):219–25. <https://doi.org/10.1038/nature11529> PMID: [23060192](https://pubmed.ncbi.nlm.nih.gov/23060192/)
31. Arichi T, Whitehead K, Barone G, Pressler R, Padormo F, Edwards AD, et al. Localization of spontaneous bursting neuronal activity in the preterm human brain with simultaneous EEG-fMRI. *elife*. 2017;6:e27814. <https://doi.org/10.7554/eLife.27814> PMID: [28893378](https://pubmed.ncbi.nlm.nih.gov/28893378/)
32. Omidvarnia A, Fransson P, Metsäranta M, Vanhatalo S. Functional bimodality in the brain networks of preterm and term human newborns. *Cereb Cortex*. 2014;24(10):2657–68. <https://doi.org/10.1093/cercor/bht120> PMID: [23650289](https://pubmed.ncbi.nlm.nih.gov/23650289/)
33. Castro Conde JR, González Campo C, González González NL, Reyes Millán B, González Barrios D, Jiménez Sosa A, et al. Assessment of neonatal EEG background and neurodevelopment in full-term small for their gestational age infants. *Pediatr Res*. 2020;88(1):91–9. <https://doi.org/10.1038/s41390-019-0693-0> PMID: [31822017](https://pubmed.ncbi.nlm.nih.gov/31822017/)
34. Moser J, Bensaid S, Kroupi E, Schleger F, Wendling F, Ruffini G, et al. Evaluating complexity of fetal MEG signals: a comparison of different metrics and their applicability. *Front Syst Neurosci*. 2019;13:23. <https://doi.org/10.3389/fnsys.2019.00023> PMID: [31191264](https://pubmed.ncbi.nlm.nih.gov/31191264/)
35. Nourhashemi M, Mahmoudzadeh M, Goudjil S, Kongolo G, Wallois F. Neurovascular coupling in the developing neonatal brain at rest. *Hum Brain Mapp*. 2020;41(2):503–19. <https://doi.org/10.1002/hbm.24818> PMID: [31600024](https://pubmed.ncbi.nlm.nih.gov/31600024/)
36. Hyvarinen A. Fast ICA for noisy data using Gaussian moments. (1999, May). In: 1999 IEEE Int Symp Circuits Syst ISCAS. IEEE. 1999: 57–61.
37. Delorme A, Makeig S. EEGLAB: an open source toolbox for analysis of single-trial EEG dynamics including independent component analysis. *J Neurosci Methods*. 2004;134(1):9–21. <https://doi.org/10.1016/j.jneumeth.2003.10.009> PMID: [15102499](https://pubmed.ncbi.nlm.nih.gov/15102499/)
38. Costa M, Goldberger AL, Peng C-K. Multiscale entropy analysis of biological signals. *Phys Rev E Stat Nonlin Soft Matter Phys*. 2005;71(2 Pt 1):021906. <https://doi.org/10.1103/PhysRevE.71.021906> PMID: [15783351](https://pubmed.ncbi.nlm.nih.gov/15783351/)
39. Lempel A, Ziv J. On complexity of finite sequences. *IEEE Trans Inf Theory*. 1976;22:75–81.
40. Willems FM, Shtarkov YM, Tjalkens TJ. The context-tree weighting method: basic properties. *IEEE Trans Inf Theory*. 1995;41(3):653–64.
41. Begleiter R, El-Yaniv R, Yona G. On prediction using variable order Markov models. *J Artif Intell Res*. 2004;22:385–421.
42. Mediano PAM, Rosas FE, Luppi AI, Noreika V, Seth AK, Carhart-Harris RL, et al. Spectrally and temporally resolved estimation of neural signal diversity. *eLife*. 2023;12:RP88683. <https://doi.org/10.7554/elife.88683.1>
43. Mediano P, Rosas F, Luppi A. EntRate: entropy rate estimators for neuroscience. 2019. <https://github.com/pmediano/EntRate>
44. O’Toole JM, Temko A, Stevenson N. Assessing instantaneous energy in the EEG: a non-negative, frequency-weighted energy operator. *Annu Int Conf IEEE Eng Med Biol Soc*. 2014;2014:3288–91. <https://doi.org/10.1109/EMBC.2014.6944325> PMID: [25570693](https://pubmed.ncbi.nlm.nih.gov/25570693/)
45. Richman JS, Moorman JR. Physiological time-series analysis using approximate entropy and sample entropy. *Am J Physiol Heart Circ Physiol*. 2000;278(6):H2039–49. <https://doi.org/10.1152/ajpheart.2000.278.6.H2039> PMID: [10843903](https://pubmed.ncbi.nlm.nih.gov/10843903/)
46. Costa M, Goldberger AL, Peng C-K. Multiscale entropy analysis of complex physiologic time series. *Phys Rev Lett*. 2002;89(6):068102. <https://doi.org/10.1103/PhysRevLett.89.068102> PMID: [12190613](https://pubmed.ncbi.nlm.nih.gov/12190613/)
47. Nikulin VV, Brismar T. Comment on “Multiscale entropy analysis of complex physiologic time series”. *Phys Rev Lett*. 2004;92(8):089803; author reply 089804. <https://doi.org/10.1103/PhysRevLett.92.089803> PMID: [14995828](https://pubmed.ncbi.nlm.nih.gov/14995828/)
48. Humeau-Heurtier A. The multiscale entropy algorithm and its variants: a review. *Entropy*. 2015;17:3110–23.
49. Ziv J. Coding theorems for individual sequences. *IEEE Trans Inf Theory*. 1978;24: 405–12.
50. Gao Y, Kontoyiannis I, Bienenstock E. Estimating the entropy of binary time series: methodology, some theory and a simulation study. *Entropy*. 2008;10:71–99.
51. Wager TD, Davidson ML, Hughes BL, Lindquist MA, Ochsner KN. Prefrontal-subcortical pathways mediating successful emotion regulation. *Neuron*. 2008;59(6):1037–50. <https://doi.org/10.1016/j.neuron.2008.09.006> PMID: [18817740](https://pubmed.ncbi.nlm.nih.gov/18817740/)
52. Wager TD, Waugh CE, Lindquist M, Noll DC, Fredrickson BL, Taylor SF. Brain mediators of cardiovascular responses to social threat: part I: reciprocal dorsal and ventral sub-regions of the medial prefrontal cortex and heart-rate reactivity. *Neuroimage*. 2009;47(3):821–35. <https://doi.org/10.1016/j.neuroimage.2009.05.043> PMID: [19465137](https://pubmed.ncbi.nlm.nih.gov/19465137/)
53. Benjamini Y, Hochberg Y. Controlling the false discovery rate: a practical and powerful approach to multiple testing. *J R Stat Soc Ser B Methodol*. 1995;57:289–300.

54. Wallois F, Routier L, Heberlé C, Mahmoudzadeh M, Bourel-Ponchel E, Moghimi S. Back to basics: the neuronal substrates and mechanisms that underlie the electroencephalogram in premature neonates. *Neurophysiol Clin.* 2021;51(1):5–33. <https://doi.org/10.1016/j.neucli.2020.10.006> PMID: [33162287](https://pubmed.ncbi.nlm.nih.gov/33162287/)
55. Feldman DP, Crutchfield JP. Measures of statistical complexity: why? *Phys Lett A.* 1998;238(4–5):244–52.
56. Sarasso S, Casali AG, Casarotto S, Rosanova M, Sinigaglia C, Massimini M. Consciousness and complexity: a consilience of evidence. *Neurosci Conscious.* 2021;2021(2):niab023. <https://doi.org/10.1093/nc/niab023> PMID: [38496724](https://pubmed.ncbi.nlm.nih.gov/38496724/)
57. Ort A, Smallridge JW, Sarasso S, Casarotto S, von Rotz R, Casanova A, et al. TMS-EEG and resting-state EEG applied to altered states of consciousness: oscillations, complexity, and phenomenology. *iScience.* 2023;26(5):106589. <https://doi.org/10.1016/j.isci.2023.106589> PMID: [37138774](https://pubmed.ncbi.nlm.nih.gov/37138774/)
58. Rolls E, Deco G. *The Noisy Brain: Stochastic Dynamics as a Principle of Brain Function.* Oxford University Press; 2010.
59. Varley TF, Luppi AI, Pappas I, Naci L, Adapa R, Owen AM, et al. Consciousness & brain functional complexity in propofol anaesthesia. *Sci Rep.* 2020;10(1):1018. <https://doi.org/10.1038/s41598-020-57695-3> PMID: [31974390](https://pubmed.ncbi.nlm.nih.gov/31974390/)
60. Mitchell M. *Complexity: A Guided Tour.* Oxford University Press; 2009.
61. Kostović I. The enigmatic fetal subplate compartment forms an early tangential cortical nexus and provides the framework for construction of cortical connectivity. *Prog Neurobiol.* 2020;194:101883. <https://doi.org/10.1016/j.pneurobio.2020.101883> PMID: [32659318](https://pubmed.ncbi.nlm.nih.gov/32659318/)
62. Moore AR, Zhou W-L, Jakovcevski I, Zecevic N, Antic SD. Spontaneous electrical activity in the human fetal cortex in vitro. *J Neurosci.* 2011;31(7):2391–8. <https://doi.org/10.1523/JNEUROSCI.3886-10.2011> PMID: [21325506](https://pubmed.ncbi.nlm.nih.gov/21325506/)
63. De Wel O, Van Huffel S, Lavanga M, Jansen K, Dereymaeker A, Dudink J, et al. Relationship between early functional and structural brain developments and brain injury in preterm infants. *Cerebellum.* 2021;20(4):556–68. <https://doi.org/10.1007/s12311-021-01232-z> PMID: [33532923](https://pubmed.ncbi.nlm.nih.gov/33532923/)
64. Bayne T, Frohlich J, Cusack R, Moser J, Naci L. Consciousness in the cradle: on the emergence of infant experience. *Trends Cogn Sci.* 2023;27(12):1135–49. <https://doi.org/10.1016/j.tics.2023.08.018> PMID: [37838614](https://pubmed.ncbi.nlm.nih.gov/37838614/)
65. Xie H-B, He W-X, Liu H. Measuring time series regularity using nonlinear similarity-based sample entropy. *Phys Lett A.* 2008;372(48):7140–6. <https://doi.org/10.1016/j.physleta.2008.10.049>
66. Fombonne E. Epidemiological surveys of autism and other pervasive developmental disorders: an update. *J Autism Dev Disord.* 2003 Aug;33(4):365–82. <https://doi.org/10.1023/A:1025054610557>
67. Grevén CU, Richards JS, Buitelaar JK. Sex differences in ADHD. In: *Oxford textbook of attention deficit hyperactivity disorder.* 2018. p. 154–60. <https://doi.org/10.1093/med/9780198739258.001.0001>
68. Garris J, Quigg M. The female Tourette patient: sex differences in Tourette disorder. *Neurosci Biobehav Rev.* 2021;129:261–8. <https://doi.org/10.1016/j.neubiorev.2021.08.001> PMID: [34364945](https://pubmed.ncbi.nlm.nih.gov/34364945/)
69. Castle DJ, Deale A, Marks IM. Gender differences in obsessive compulsive disorder. *Aust N Z J Psychiatry.* 1995;29(1):114–7. <https://doi.org/10.3109/00048679509075899> PMID: [7625960](https://pubmed.ncbi.nlm.nih.gov/7625960/)
70. Varley TF, Sporns O, Stevenson NJ, Yrjölä P, Welch MG, Myers MM, et al. Emergence of a synergistic scaffold in the brains of human infants. *Commun Biol.* 2025 May 13;8(1):743. <https://doi.org/10.1038/s42003-025-08082-z>
71. Jeste SS, Frohlich J, Loo SK. Electrophysiological biomarkers of diagnosis and outcome in neurodevelopmental disorders. *Curr Opin Neurol.* 2015;28(2):110–6. <https://doi.org/10.1097/WCO.000000000000181> PMID: [25710286](https://pubmed.ncbi.nlm.nih.gov/25710286/)
72. Shanker A, Abel JH, Schamberg G, Brown EN. Etiology of burst suppression EEG patterns. *Front Psychol.* 2021;12:673529. <https://doi.org/10.3389/fpsyg.2021.673529> PMID: [34177731](https://pubmed.ncbi.nlm.nih.gov/34177731/)